Koch-Müller, M., Rhede, D. (2010): IR absorption coefficients for water in nominally anhydrous high-pressure minerals. - American Mineralogist, 95, 770-775

DOI: 10.2138/am.2010.3358

American Mineralogist, Volume 95, pages 770–775, 2010

IR absorption coefficients for water in nominally anhydrous high-pressure minerals

Monika Koch-Müller[1,*] and Dieter Rhede[2]

[1]Sektion 3.3, Chemie und Physik der Geomaterialien, Deutsches GeoForschungsZentrum, Telegrafenberg, D-14473 Potsdam, Germany
[2]Sektion 4.2, Anorganische und Isotopengeochemie, Deutsches GeoForschungsZentrum, Telegrafenberg, D-14473 Potsdam, Germany

Abstract

Infrared spectroscopic quantification of traces of OH and H_2O in minerals and glasses is based on the Beer Lambert law $A = \varepsilon \cdot c \cdot t$, where ε is the molar absorption coefficient. Numerous experimental and theoretical studies show that ε generally increases with decreasing wavenumbers. However, this general trend seems to be valid only for hydrous minerals and glasses and should not be applied to water quantification in nominally anhydrous minerals (NAMs) that incorporate traces of water in their structures. In this study, we analyze ε-values from literature data and propose that within a polymorphic mineral series of the same composition ε negatively correlates with the molar volume and positively correlates with the density of the respective mineral phase. To test this hypothesis, we determined ε-values for synthetic hydrous ringwoodite samples ranging in composition from $X_{Mg} = 0.0$ to 0.6 by combining results of FTIR-spectroscopy with those of secondary ion mass spectrometry. The ε-values plot well below the general calibration curves but follow the same trend, i.e., they increase with decreasing wavenumbers of the OH bands from 59 000 ± 6000 for the Fe end-member to 85 800 ± 10 000 L/mol(H_2O)/cm^{-2} for the Mg-richest sample. From this relation we can predict an absorption coefficient for the iron-free Mg end-member as 100 000 ± 7000 L/mol(H_2O)/cm^{-2}. This value together with ε-values for forsterite and wadsleyite taken from literature confirm the proposed correlation with the molar volume and density within this polymorphic series. This allows us to predict absorption coefficients for some minerals, where coefficients for one or better two of their polymorphs, either high- or low-pressure, are available.

Keywords: Infrared spectroscopy, absorption coefficient, ringwoodite, nominally anhydrous minerals

Introduction

Infrared spectroscopy is a powerful tool to determine the presence of OH and H_2O in minerals and glasses. The application is based on the Beer Lambert law $A = \varepsilon \cdot c \cdot t$, where A is the absorbance, ε the molar absorption coefficient, e.g., in L/mol(H_2O)/cm^{-2}, the concentration in mol/L and t the thickness in centimeters. The molar absorption coefficient ε can be given as the linear absorption coefficient in L/mol(H_2O)/cm^{-1} using the peak height as measure for the absorption or as the integral absorption coefficient ε_i [in L/mol(H_2O)/cm^{-2}] when the area under the corresponding OH bands is considered[1]. Figure 1a shows the trend for absorption coefficients ε_i for water in hydrous minerals and glasses vs. the wavenumber of the corresponding OH-bands as determined experimentally by Paterson (1982) and Libowitzky and Rossman (1997), and as calculated theoretically in the studies of Kubicki et al. (1993) and Balan et al. (2008). There is no doubt about the general trend, i.e., that ε increases with decreasing wavenumber. Although this trend is expected theoretically, the absolute values of the different calibrations cover a broad field. The deviations between the calibration curves of the four studies increase with decreasing wavenumber. We regard the calibration curve of Libowitzky and Rossman (1997) as most reliable because the curve is based on direct measurements of many samples. However, it has been observed that the general trend of increasing ε with decreasing wavenumber is valid only for hydrous minerals and glasses and should not be applied to water quantification in nominally anhydrous minerals (NAMs), which incorporate traces of water in their structures (e.g., Rossman 2006; Thomas et al. 2009). For example, Bell et al. (2003) showed that if the general IR calibration of Paterson (1982) is adopted, the water concentration of olivine is underestimated by about 25%. Deon et al. (2010) obtained a similar result for Mg-wadsleyite. Thomas et al. (2009) used many various analytical methods to show that if mineral-specific IR-calibrations for the OH quantification in NAMs are not applied, this can lead to either underestimation of the water content in some minerals, e.g., olivine, or overestimation of the water content in other minerals, e.g., stishovite and coesite. Thus, to quantify the water content of NAMs, mineral-specific molar absorption coefficients are needed. Unfortunately, these data are only available for a few minerals.

In this study, we examined literature data of ε for NAMs and determined ε for synthetic hydrous ringwoodites. We found that within a polymorphic series, e.g., SiO_2 or Mg_2SiO_4, ε increases with increasing density and decreasing molar volume.

* E-mail: mkoch@gfz-potsdam.de

[1]In some studies, e.g., in Paterson (1982), ε for OH bands is not given per mole H_2O but per mole H. In Figure 1, some original values are recalculated so that they all are shown as ε for H_2O.

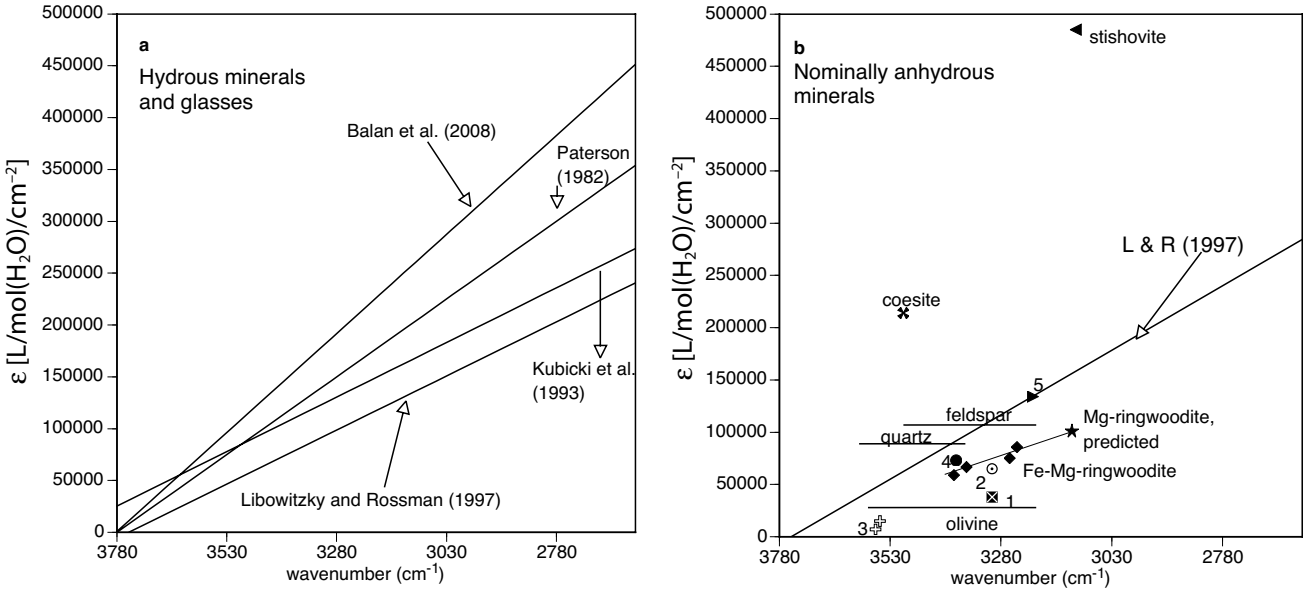

FIGURE 1. (**a**) General trend of ε-values for water in hydrous minerals and glasses vs. wavenumbers of the corresponding OH bands as determined experimentally by Paterson (1982) and Libowitzy and Rossman (1997) and as calculated in theoretical studies by Kubicki et al. (1993) and Balan et al. (2008); in respect to the correlations by Paterson (1982) and Libowitzy and Rossman (1997), only the idealized trends are shown for simplicity—in reality the data scatter a bit around these trends. (**b**) Comparison of the general trend of ε-values for water in hydrous minerals and glasses vs. wavenumbers of the corresponding OH bands as determined experimentally by Libowitzy and Rossman (1997) with ε-values for NAMs from literature and for Fe-Mg ringwoodite determined in this study. Labels: 1, 2 = rutile and cassiterite, respectively (Maldener et al. 2001); 3 = garnets (Maldener et al. 2003); 4 = Mg wadsleyite (Deon et al. 2010); 5 = r-GeO_2 (Thomas et al. (2009). From the trend observed for Fe-Mg ringwoodite a ε-value for the Fe-free Mg end-member ringwoodite can be predicted (star symbol).

EXPERIMENTAL METHODS

Syntheses and electron microprobe

Experiments to synthesize ringwoodite were performed in a multi-anvil apparatus at 7 and 13 GPa and 1000–1200 °C. We synthesized four ringwoodite compositions, with X_{Mg} = 0.00, 0.22, 0.39, and 0.60. For quantitative chemical analyses, the samples were embedded in a minimum amount of epoxy resin, polished, and analyzed using a JEOL thermal field emission type electron-probe JXA-8500F (HYPERPROBE). Details regarding the syntheses and microprobe analyses are given in Koch-Müller et al. (2009). The crystal size decreases with increasing Mg content from about 500 µm for the Fe end-member, which appears opaque, to about 30 µm or less for the most Mg-richest sample (X_{Mg} = 0.60), which shows a blue color (see Taran et al. 2009).

FTIR spectroscopy

Several crystals of each sample were prepared for FTIR measurements. The crystals were polished from two sides as wafers about 20–30 µm thick; crystal wafers of sample MA120 were about 20 µm thick. Unpolarized FTIR spectra were measured with a Bruker IFS66v FTIR spectrometer connected to a Hyperion microscope. We used a Globar light source, a KBr beamsplitter, and an InSb detector. The spectra were collected with a resolution of 2 cm^{-1} and averaged over 256 scans in the OH-stretching region between 2500 and 4000 cm^{-1}. The molar absorption coefficient, ε [L/mol(H_2O)/cm^{-2}], was calculated using the Beer-Lambert relation with $A_{i,tot}$ as the mean value of the total integrated intensities (cm^{-1}) of the unpolarized measurement multiplied by three (see Libowitzky and Rossman 1996). The water concentration (wt%) was measured with secondary ion mass spectrometry (SIMS) (see below). We integrated the area under the broad IR absorption band that shifts with increasing Mg content to lower wavenumber, from 3386 cm^{-1} for the Fe end-member to 3244 cm^{-1} for the ringwoodite with X_{Mg} = 0.6. There is another absorption feature in the range 2500–2700 cm^{-1} that we excluded from the water quantification as it has been assigned as overtone ($2\nu_3 + 2\nu_4$) by Hofmeister and Mao (2001). All spectra were fitted with the program PeakFit by Jandel Scientific (version 4.11) using the second derivative zero algorithm for the background and a mixed Gaussian and Lorenzian distribution function for the component bands. The algorithm for the background fitting is unique to PeakFit and was applied in the spectral range 2500–4000 cm^{-1}. The algorithm is based on the fact that baseline points tend to exist where the second derivative of the data are both constant and zero.

Secondary ion mass spectrometry

The ^1H content of the crystals was measured by SIMS using a CAMECA ims 6f ion probe. Before each session, the instrument was baked for at least 48 h. The vacuum was achieved by using a permanent filling liquid nitrogen trap, which ensured that the total vacuum pressure in the sample chamber during the analysis was always better than 4 10^{-8} Pa. Samples were prepared as described in the EMPA section. For SIMS measurement the samples were cleaned in an ultrasonic bath with pure ethanol, stored in an oven at 70 °C then covered with an approximately 30 nm high pure gold layer and put in the airlock chamber at a pressure better than 310^{-7} Pa for more than three days. We prepared and measured only clear single crystals free of cracks to ensure that only intrinsic H from the ringwoodite samples was determined. The primary beam of $^{16}O^-$ ions was accelerated to 12.5 kV, the beam current was set to 2 nA, and the beam was focused to a ~10 µm diameter on the sample surface. Prior to each spot analysis the surface was cleaned by pre-sputtering a 40 × 40 µm area for 120 s. Positive secondary ions were extracted using a potential of 10 kV and the energy slit was placed at a width equal to 50 eV. A 150 µm contrast aperture and a 400 µm field aperture ensured that only ions from the central part of the pre-sputtered area were counted. The mass resolution was (M/ΔM) = 3000, which is sufficient to eliminate all isobaric interferences. Counting times per cycle were 15 s for ^1H and 2 s for ^{30}Si. The average acquisition time was 70 min and the $^1H/^{30}Si$ ratios were calculated by averaging only the last 100 cycles from each analysis. To build the calibration curves of the $^1H/^{30}Si$ ratios, well-characterized hydrous Mg end-member wadsleyite and garnets were used as reference materials. Water contents of these standards were measured with independent techniques (Deon et al. 2010; Maldener et al. 2003, respectively).

RESULTS

In Figure 1b, ε-values of some NAMs from the literature are shown, together with the calibration curve of Libowitzky and Rossman (1996). Thomas et al. (2009) discussed how ε-values for NAMs cannot be estimated using the general calibration

line—the values plot above and below the curve of Libowitzky and Rossman (1996). The most important features of Figure 1b are (1) that ε in the system SiO_2 increases from quartz to coesite to stishovite, thus with increasing density, and (2) that different OH-defects in feldspar (Johnson and Rossman 2003) as well as in olivine and quartz (Thomas et al. 2009) have single ε-values that are independent of wavenumber. Figure 1b also shows the data obtained in this study for synthetic hydrous ringwoodite. The composition, water contents, and spectroscopic details of the four synthetic ringwoodite samples are given in Table 1. The hydroxyl content expressed as wt% water increases with increasing Mg content from 0.21 to 0.36 wt%. In all samples, water was added in excess and was still present after quenching. Infrared spectra in the OH-stretching range of the four synthetic ringwoodite samples are shown in Koch-Müller et al. (2009)[2]. The ε-values of the four different ringwoodite samples plot well below the general calibration curve of Libowitzky and Rossman (1997) but follow the same trend, i.e., they increase with decreasing wavenumber of the OH bands (Fig. 1b).

Discussion

The general trend of the calibration curve shown in Figure 1 is expected, based on the following arguments. OH bands observed in infrared spectra of solids can occur over a broad energy range from about 3800 cm^{-1} to values down to 1000 cm^{-1}, depending on the strength of the OH dipole and the H-bonding in the O1-H···O2 arrangement. For an OH-band in the high energy range of the OH-stretching vibration, e.g., around 3700 cm^{-1}, as in brucite [$Mg(OH)_2$], the OH dipole is very strong with an O1-H distance of 0.945 Å and H-bonding does not exist as the H···O2 distance is large, i.e., 3.84 Å (structural data from Zhukhlistov et al. 1997). In contrast, in pectolite [$NaCa_2Si_3O_8(OH)$] that shows an OH-band around 1000 cm^{-1} (Libowitzky and Rossman 1997), the hydroxyl dipole is rather weak with a distance of 1.061 Å and H-bonding is strong as the H1···O2 distance is only 1.42 Å (structural data from Takeuchi and Kudoh 1977). Thus, with increasing hydrogen bonding, the corresponding OH band shifts to lower wavenumbers. Simultaneously, the intensities of the OH bands in infrared spectra increase with decreasing wavenumber. Infrared intensities depend on the square of the dipole moment derivative. The dipole moment is defined as the product of the magnitude of the charge on the atoms and the distance between the two bonded atoms. Increasing hydrogen bonding to O2 affects the dipole moment of the OH group as the O1-H distance increases and thus the intensity of the corresponding OH band in the infrared spectrum.

The problem with understanding OH incorporation in NAMs is, however, that the geometry of the structural defects is not known and hence the distances and angles of the O1-H1···O2 environments are also unknown. It may be that the correlation of the O-H stretching frequencies and the O-H···O hydrogen bond lengths cannot be applied for NAMs. However, even if only traces of OH are incorporated, the general law that the intensity of the OH-bands increases with increasing dipole moment must be valid. Bulk properties of minerals may contain some information on the structure and geometry of the defects. Looking at the ε-values for the system SiO_2 (Fig. 1b), i.e., quartz and its high-pressure polymorphs coesite and stishovite, there is a strong increase of ε from quartz to stishovite—much stronger than one would deduce from the general calibration curves for hydrous minerals. Thomas et al. (2009) interpreted this observation in terms of an increase of the densities (ρ) of the structures that leads to a decrease of the O-O distances from quartz to stishovite. Indeed Figure 2a shows the correlation between ε and density for the system SiO_2. Starting from the value of quartz, ε for the high-pressure phases increases as the overall band distances decrease, while the magnitude of the OH dipole moment increases. Another bulk property that contains information on the bond distances is the molar volume. Figure 2b shows that ε for the system SiO_2 increases with decreasing molar volume. The advantage of using the molar volume instead of density is that it also works for systems with different compositions, because it is less dependent on composition. Figures 2c and 2d show minerals with rutile structure but different compositions such as SiO_2, GeO_2, TiO_2, and SnO_2: there is no correlation of ε with density, but a fairly good correlation of ε with molar volume. Thus, we propose that for NAMs with the same composition, the bulk properties molar volume and density somehow reflect the geometry of the OH defects, and correspondingly the magnitude of ε. This is consistent with the observation that different defects in feldspar (Johnson and Rossman 2003), as well as in olivine and quartz (Thomas et al. 2009), have single ε-values that are independent of wavenumber (Fig. 1b), because the densities and molar volumes of the bulk structures in each case are very similar.

[2]In Koch-Müller et al. (2009), the normalized IR spectrum for sample MA121 (Fig. 5a) is not correct. We realized later that the sample was too thick, resulting in saturation of the absorbance.

Table 1. Characteristics of the Fe-Mg ringwoodite crystals synthesized in this study

	X_{Mg}	$A_{i,tot}$ (mm^{-1})	wavenumber (cm^{-1})	water wt%	$\varepsilon_{i,tot}$ this study [L/mol(H_2O)/cm^{-2}]	$\varepsilon_{i,tot}$ L&R* [L/mol(H_2O)/cm^{-2}]	molar volume (cm^3/mol)	density (g/cm^3)
MA75	0.00	3200	3386	0.21(1)	59 000 (6000)	90 435	42.14	4.87
MA56	0.22	3144	3358	0.19(2)	66 600 (10 000)	97 385	41.65	4.56
MA62	0.39	5682	3260	0.30(2)	75 300 (10 000)	121 697	41.11	4.36
MA120	0.60	6909	3244	0.36(3)	85 800 (10 000)	125 560	40.52	4.09
Mg-ringwoodite predicted	1.00		3120		104 692† 105 877‡ 90 762§ 100 000‖	160 000		

* L&R: Libowitzky and Rossman (1997).
† Estimated from a linear fit of ε from MA75 to MA120 vs. wavenumber.
‡ Estimated from a linear fit of ε from MA75 to MA120 vs. density.
§ Estimated from a linear fit of ε from MA75 to MA120 vs. molar volume.
‖ Average of the three estimated values.

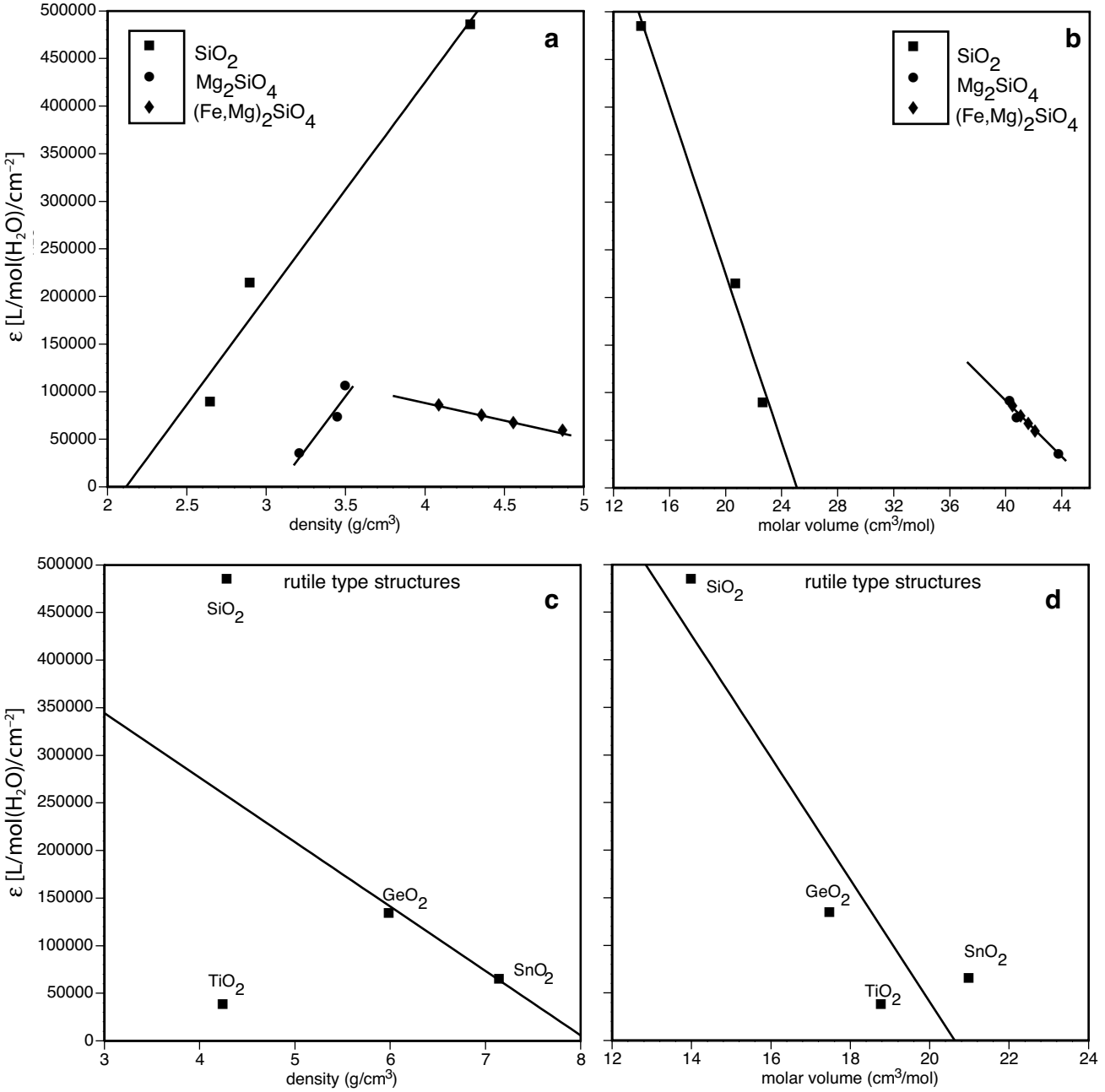

FIGURE 2. Plot of ε-values vs. density and molar volume (for references see Table 2) (**a** and **b**) for the system SiO_2, the polymorphs of Mg_2SiO_4, and ringwoodite solid solutions $(Fe,Mg)_2SiO_4$; the solid line in **b** through the symbols is only a guide for the eye; (**c** and **d**) for rutile type structures.

To test our hypothesis, we investigated the relationships between ε, density, and molar volume in synthetic hydrous ringwoodite. Our data show that applying the general IR calibration of Libowitzky and Rossman (1997) to water determination in ringwoodite underestimates the water content (Fig. 1b). Such behavior was predicted by Blanchard et al. (2009) in a computational study: they found that water in Fe-free ringwoodite might be underestimated by about 20% compared to the theoretically deduced general calibration law given by Balan et al. (2008). From the trend of ε of the synthetic ringwoodite samples with decreasing wavenumber (Fig. 1b), we can predict a molar absorption coefficient for the Mg end-member with an OH-band maximum at 3120 cm^{-1} (e.g., Bolfan-Casanova et al. 2000) as 101 613 $[L/mol(H_2O)/cm^{-2}]$. Libowitzky and Rossman's calibration would give a much higher value of about 156 000 $[L/mol(H_2O)/cm^{-2}]$.

Figures 2a and 2b show ε-values as a function of density and molar volume for the synthetic ringwoodite, together with values for SiO_2 and Mg_2SiO_4 polymorphs. As expected, the ε-values of ringwoodite do not increase with increasing density, because of the change in composition. Instead, there is a linear negative correlation between the ε-values and the densities. We can use this relationship to predict a ε-value for Mg end-member ringwoodite (density 3.5 g/cm^3) of 105 877 $[L/mol(H_2O)/cm^{-2}]$. This value is close to the value predicted by the wavenumber dependence of

TABLE 2. Absorption coefficients, volume and density data of selected minerals

	$\varepsilon_{i,tot}$ [L/mol(H_2O)/cm^{-2}]	Ref. for $\varepsilon_{i,tot}$	Molar volume (cm^3/mol)	Density (g/cm^3)
wadsleyite	73 000	Deon et al. (2010)	40.80	3.45
forsterite	35 000	Thomas et al. (2009)	43.94	3.21
orthopyroxene*	80 600	Bell et al. (1995)	39.90	3.32
clinopyroxene	110 000†	predicted this study	29.36	3.42
	160 000‡			
akimotoite	170 000†	predicted this study	26.35	3.81
	190 000‡			
perovskite	220 000	predicted this study	24.47	4.10
post-stishovite	480 000	predicted this study	13.97	4.30
stishovite	485 000	Thomas et al. (2009)	14.01	4.29
coesite	214 000	Thomas et al. (2009)	20.75	2.90
quartz	89 000	Thomas et al. (2009)	22.68	2.65
tridymite	30 000	predicted this study	26.13	2.28
rutile	38 000	Maldener et al. (2001)	18.79	4.25
anatase	15 000	predicted this study	20.60	3.88
cassiterite	65 000	Maldener et al. (2001)	21.07	7.15
r-GeO_2	134 000	Thomas et al. (2009)	17.46	5.99
GeO_2 (quartz)	35 000	predicted this study	24.39	4.29
GeO_2 ($CaCl_2$)	180 000	predicted this study	15.08	6.94
oligoclase $Ab_{67}An_{24}Or_8$	117 955§	Johnson and Rossman (2003)	100.23	2.64
microcline Ab_6Or_{94}	91 835§	Johnson and Rossman (2003)	108.5	2.56
K-hollandite	250 000	predicted this study	71.40	3.90
Na-hollandite	265 000	predicted this study	69.00	3.80
kyanite	32 900	Bell et al. (2004)	44.18	3.67
andalusite	20 000	predicted this study	49.88	3.25
sillimanite	15 000	predicted this study	51.51	3.15

* $(Mg_{0.85}Fe_{0.1}Al_{0.05})SiO_3$.
† Estimated from density.
‡ Estimated from molar volume.
§ Calculated according to the data of Johnson and Rossman (2003).

ε given above. However, as outlined before, if we want to look at the effect of a denser structure on the ε-values, only minerals with similar compositions should be compared, such as the SiO_2 system with data for quartz, coesite, and stishovite. Taking the predicted value for Mg-ringwoodite and experimental data from Table 2 for forsterite (Thomas et al. 2009) and Mg-wadsleyite (Deon et al. 2010), we obtain the expected relationship for the Mg_2SiO_4 system (Fig. 2a). The slope $d\varepsilon/d\rho$ for the system Mg_2SiO_4 is nearly the same as for the system SiO_2. As discussed above, a better comparison can be achieved if the ε-values are plotted against the molar volume as shown in Figure 2b. There is a linear relationship between the molar volume and ε for the ringwoodite solid solution. If we extrapolate this relation to the molar volume of Mg-ringwoodite, ε would be 90 700 [L/mol(H_2O)/cm^{-2}]. Taking an average value from all the predicted ε-values of Mg-ringwoodite from this study, i.e., 100 000 [L/mol(H_2O)/cm^{-2}], one obtains again a linear relation between ε of the Mg_2SiO_4 polymorphs and their molar volumes (Table 2).

On the basis of these correlations, we can predict ε-values for minerals where coefficients for one or preferably two of their polymorphs, either high- or low-pressure, are available. Examples are shown in Figure 3, with data given in Table 2, and include the following: (1) the system SiO_2, where we predict ε-values for tridymite and post-stishovite based on ε-values of quartz, coesite, and stishovite (Thomas et al. 2009); (2) the system Mg_2SiO_4 that has been discussed above; (3) the system Al_2SiO_5, where we predict ε-values for andalusite and sillimanite based on the ε-values of kyanite (Bell et al. 2004); (4) the system GeO_2, where we predict ε-values for GeO_2 in quartz structure and GeO_2 in $CaCl_2$-structure based on the ε-values of r-GeO_2 (Thomas et al. 2009); (5) the system TiO_2 where we predict an ε-value for anatase based on the ε-values of rutile (Maldener et al. 2001); (6) the system $(K,Na)AlSi_3O_8$ where we predict ε-values for K- and Na-hollandite based on the ε-values of oligoclase and microcline (Johnson and Rossman 2003)[3]; and finally (7) for the system $MgSiO_3$, where we predict ε-values for clinopyroxene, akimotoite, and perovskite based on the ε-value of orthopyroxene (Bell et al. 1995).

To summarize our findings, we suggest that the bulk properties molar volume and density of NAMs with the same composition somehow reflect the geometry of OH defects and corresponding changes in the dipole moment. Different to hydrous minerals, OH in NAMs is incorporated via point defects with unusual and often unknown O-H···O environments for charge balancing and the chemical and electric fields around these defects may play an important role for the absorptivity of an OH band. The magnitude of ε within a polymorphic series is strongly influenced by the density and molar volume of the polymorphs. These conclusions are based on the following observations: (1) ε in the simple systems SiO_2 and Mg_2SiO_4 increases with increasing density and decreasing molar volume, independent of the nature of the OH defects; (2) different defects in feldspar (Johnson and Rossman 2003) as well as in olivine and quartz (Thomas et al. 2009) have single ε-values independent of wavenumber because the densities and molar volumes of the bulk structures of the respective minerals were very similar; (3) ε-values for some minerals in rutile-structure of the systems SiO_2, GeO_2, TiO_2, and SnO_2 correlate with their molar volumes; and (4) ε of Fe-Mg ringwoodite samples is wavenumber dependent as the ringwoodites strongly differ—through the substitution of iron

[3]Johnson and Rossman (2003) gave a single ε-value for feldspar independent on composition. From their original data, we calculated individual ε-values.

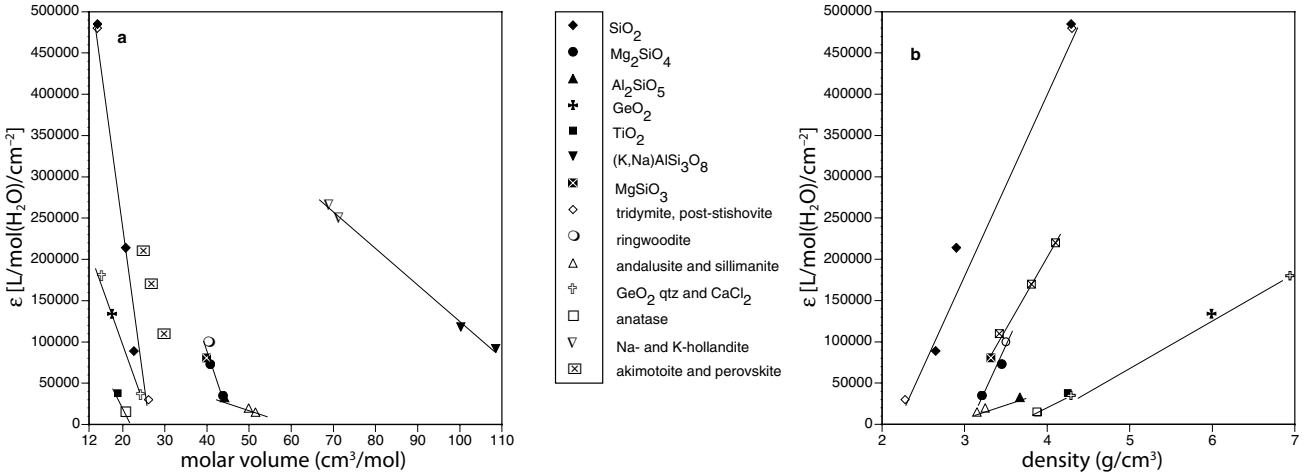

FIGURE 3. Plot of ε-values vs. molar volume (**a**) and density (**b**): the closed symbols are taken from literature and the same symbols, but open are estimated values for the respective high- or low-pressure polymorphs; for references see Table 2.

by magnesium—in their interatomic distances that is reflected more in the density than in the molar volume.

ACKNOWLEDGMENTS

We thank G. Berger and I. Schäpan for their technical support. A first draft of this article was discussed with S. Jahn, E. Libowitzky, and W. Heinrich for which we are thankful. Many thanks also to the associate editor R. Jones and the reviewers G.R. Rossman and A.M. Hofmeister.Their comments and suggestions helped to improve the manuscript.

REFERENCES CITED

Balan, E., Refson, K., Blanchard, M., Delattre, S., Lazzeri, M., Ingrin, J., Mauri, F., Wright, K., and Winkler, B. (2008) Theoretical infrared absorption coefficient of OH groups in minerals. American Mineralogist, 93, 950–953.

Bell, D.R., Ihinger, P.H., and Rossman, G.R. (1995) Quantitative analysis of trace OH in garnet and pyroxenes. American Mineralogist, 80, 465–474.

Bell, D.R., Rossman, G.R., Maldener, J., Endisch, D., and Rauch, F. (2003) Hydroxide in olivine: a quantitative determination of the abslute amount and calibration of the IR spectrum. Journal of Geophysical Research B: Solid Earth and Planets, 108, 2105, DOI: 10.1029/2001JB000679.

Bell, D.R., Rossman, G.R., Maldener, J., Endisch, D., and Rauch, F. (2004) Hydroxide in kyanite: A quantitative determination of the absolute amount and calibration of the IR spectrum. American Mineralogist, 89, 998–1003.

Blanchard, M., Balan, E., and Wright, K. (2009) Incorporation of water in iron-free ringwoodite: A first-principles study. American Mineralogist, 94, 83–89.

Bolfan-Casanova, N., Keppler, H., and Rubie, D.C. (2000) Water partitioning between nominally anhydrous minerals in the MgO-SiO_2-H_2O system up to 24 GPa: Implications for the distribution of water in the Earth's mantle. Earth and Planetary Science Letters, 182, 209–221.

Deon, F., Koch-Müller, M., Rhede, D., Gottschalk, M., Wirth, R., and Thomas, S.-M. (2010) Location and quantification of hydroxyl in wadsleyite: New insights. American Mineralogist, 95, 312–322.

Hofmeister, A.M. and Mao, H.K. (2001) Evaluation of shear moduli and other properties of silicates with the spinel structure from IR spectroscopy. American Mineralogist, 86, 622–639.

Johnson, E.A. and Rossman, G.R. (2003) The concentration and speciation of hydrogen in feldspars using FTIR and ^{1}H MAS NMR spectroscopy. American Mineralogist, 88, 901–911.

Koch-Müller, M., Rhede, D., Schulz, R., and Wirth, R. (2009) Breakdown of hydrous ringwoodite to pyroxene and spinelloid at high *P* and *T* and oxidizing conditions. Physics and Chemistry of Minerals, 36, 324–341.

Kubicki, J.D., Sykes, D., and Rossman, G.R. (1993) Calculated trends of OH infrared stretching vibrations with composition and structure in aluminosilicate molecules. Physics and Chemistry of Minerals, 20, 425–432.

Libowitzky, E. and Rossman, G.R. (1996) Principles of quantitative absorbance measurements in anisotropic crystals. Physics and Chemistry of Minerals, 23, 319–327.

——— (1997) An IR absorption calibration for water in minerals. American Mineralogist, 82, 1111–1115.

Maldener, J., Rauch, F., Gavranic, M., and Beran, A. (2001) OH absorption coefficients of rutile and cassiterite deduced from nuclear reaction analysis and FTIR spectroscopy. Mineralogy and Petrology, 71, 21–29.

Maldener, J., Hösch, A., Langer, K., and Rauch, F. (2003) Hydrogen in some natural garnets studied by nuclear reaction analysis and vibrational spectroscopy. Physics and Chemistry of Minerals, 30, 337–344.

Paterson, M.S. (1982) The determination of hydroxyl by infrared absorption in quartz, silicate glasses and similar materials. Bulletin de Minéralgie, 105, 20–29.

Rossman, G.R. (2006) Analytical methods for measuring water in nominally anhydrous minerals. In H. Keppler and J.R. Smyth, Eds., Water in nominally anhydrous minerals, 62, p. 1–28. Reviews in Mineralogy and Geochemistry, Mineralogical Society of America, Chantilly, Virginia.

Takeuchi, Y. and Kudoh, Y. (1977) Hydrogen bonding and cation ordering in Magnet Cove pectolite. Zeitschrift für Kristallographie, 146, 281–292.

Taran, M., Koch-Müller, M., Wirth, R., Abs-Wurmbach, I., Rhede, D., and Greshake, A. (2009) Spectroscopic studies of synthetic and natural ringwoodite, γ-$(Mg, Fe)_2SiO_4$. Physics and Chemistry of Minerals, 36, 217–232.

Thomas, S.-M., Koch-Müller, M., Reichart, P., Rhede, D., Thomas, R., Wirth, R., and Matsyuk, S. (2009) IR calibrations for water determination in olivine, r-GeO_2 and SiO_2 polymorphs. Physics and Chemistry of Minerals, 36, 489–509.

Zhukhlistov, A.P., Avilov, A.S., Ferraris, D., Zvyagin, B.B., and Plotnikov, V.P. (1997) Statistical distribution of hydrogen over three positions in the brucite $Mg(OH)_2$ structure from electron diffractometry data. Crystallography Reports, 42, 774–777.

MANUSCRIPT RECEIVED JULY 28, 2009
MANUSCRIPT ACCEPTED JANUARY 27, 2010
MANUSCRIPT HANDLED BY RHIAN JONES